Calorimetric measurement methodology for comprehensive soft and hard switching loss characterisation

Beczkowski, Szymon Michal; Zäch, Mike Robin; Ahmad, Faheem; Aunsborg, Thore Stig; Munk-Nielsen, Stig

Published in:
2023 IEEE Energy Conversion Congress and Exposition, ECCE 2023

DOI (link to publication from Publisher):
10.1109/ECCE53617.2023.10362588

Publication date:
2023

Document Version
Accepted author manuscript, peer reviewed version

Calorimetric measurement methodology for comprehensive soft and hard switching loss characterisation

Szymon Bęczkowski
AAU Energy
Aalborg University
Aalborg, Denmark
sbe@energy.aau.dk

Mike Zäch
AAU Energy
Aalborg University
Aalborg, Denmark
mrz@energy.aau.dk

Faheem Ahmad
AAU Energy
Aalborg University
Aalborg, Denmark
faah@energy.aau.dk

Thore Stig Aunsborg
AAU Energy
Aalborg University
Aalborg, Denmark
tsu@energy.aau.dk

Stig Munk-Nielsen
AAU Energy
Aalborg University
Aalborg, Denmark
smn@energy.aau.dk

***Abstract*—Accurate measurement of soft and hard switching losses is challenging. Electrical methods are prone to errors and calorimetric measurements most often cannot separate turn-on and turn-off energies. We present a calorimetric test setup capable of measuring and separating turn-on and turn-off energies in soft and hard switching regimes. The resulting loss map can be used to accurately predict power semiconductor losses, even when the converter is not fully in the soft-switching regime.**

***Index Terms*—switching loss, calorimetry, power MOSFET, power transistors, zero voltage switching, soft switching**

I. Introduction

Accurate loss models are crucial when designing a power converter. With better converter model accuracy we can obtain faster time to market by spending less time on design iterations.

A crucial part of the loss budget is the switching losses of power semiconductors. These losses depend on many factors, such as external gate circuitry, layout of the power switching loop, and instantaneous junction temperature. Moreover, these losses are strongly dependent on parameters that have an inherent spread due to manufacturing issues and lifetime parameter drift, most notably gate threshold voltage [1].

High-power converters usually try to operate, at least partially, within soft switching regime. That allows the converter to minimise its switching losses and increase the switching frequency, and yields additional system benefits. Often, however, it is not possible to achieve full soft-switching within all desired operating points. Therefore, a good loss model should predict semiconductor losses in both hard and soft switching regimes, including incomplete soft-switching.

Loss models based on analytical equations exist but they are often complex and strongly depend on assumptions and simplifications [2]. Direct loss measurements are often preferred to analytical models. These, however, are relatively complex, prone to methodological errors, and often require changes to the switching setup (that impact the actual losses).

The golden standard for switching loss measurement is clamped inductive double pulse test. In this test the current in the device under test (DUT) is ramped up to a desired value and afterwards turn-off and turn-on events are electrically measured. This setup requires high-bandwidth voltage and current probes that measure the actual switching waveforms. These two probes need to be time deskewed not to introduce errors. The placement and signal fidelity of the current probe is of utmost importance, therefore a high-bandwidth current shunt is most commonly used. The switching energies must then be extracted from the time-domain voltage and current signals. The exact beginning and end of switching waveform is arbitrary and may differ between manufacturers and transistor technologies.

The results of the double pulse test often misattribute a portion of the measured turn-off energy as turn-off loss, where in practice, that energy is stored in the C_{oss} [3]. For hard-switched applications this misattribution may not be important, as this energy is dissipated in the next turn-on event, so the sum of E_{on} and E_{off} is preserved. Without the C_{oss} correction these measurements can only accurately predict losses in the hard-switched converters.

Calorimetric test setups aim to break away from problems of electrical domain sensing by (in)directly measuring the losses of the semiconductors. These methods sense the thermal domain, which means the DUT must be thermally decoupled from other semiconductors. Separation of E_{on} and E_{off} is often impossible in these setups [4], which means the results cannot be generalised. Sometimes changes need to be made to the commutation loop to facilitate the method [5].

Anderson et al. presented a calorimetric measurement method capable of differentiating the E_{on} and E_{off} energies and operating in a standard full-bridge configuration [6]. They use two variations of the same circuit, with two different inductor values, to extract the switching energies in both hard and soft switching conditions. Their method uses switching frequency control as a means of controlling the junction temperature of the DUT. We believe that their study is the most comprehensive approach to measuring and separating the turn-on and turn-off energies using a calorimetric method applicable to a non-modified commutation loop presented in the literature.

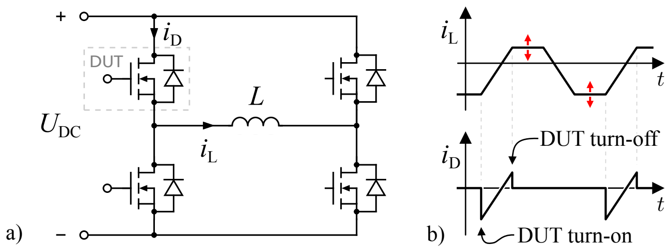

Fig. 1. a) Test circuit with the DUT b) Inductor and DUT currents.

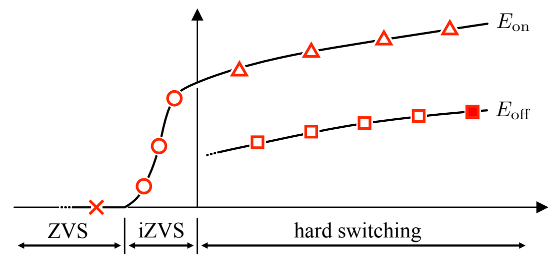

Fig. 2. Qualitative shape of the turn-on and turn-off energies of a power MOSFET.

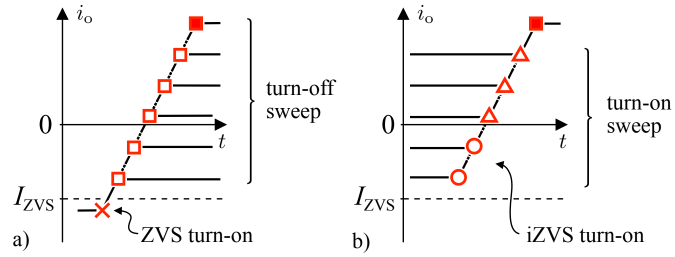

Fig. 3. Switching patterns used to measure: a) turn-off losses and b) turn-on losses. Note that the turn-off energy denoted with a filled square marker is used in the turn-on energy sweep.

There are, however, possible problems in their study not sufficiently explained in the methodology section. At low current levels, when the turn-on event falls in an incomplete soft switching regime (measured with soft-switching inductor in the setup), losses in the turn-on may be falsely attributed to hard turn-off energy. In consequence, hard turn-on data at low current levels (measured with hard-switching inductor in the setup) may be overestimated while corresponding hard turn-off losses at low current levels may be underestimated.

II. Proposed Methodology

Our approach builds on the work of Anderson et al. and extends it to measure incomplete zero-volt switching (iZVS). Their approach uses a full bridge circuit where the current in the inductor controls the switching current magnitudes (fig.1a). We propose to add a DC component to the inductor current waveform, similar to the approach by Keuck et. al. [7]. That allows to control the DUT turn-on and turn-off currents separately (fig.1b). We can then guarantee full ZVS turn-on of the DUT when estimating the turn-off losses. The added DC component makes it possible to extend the measurement into negative turn-on and turn-off currents to explore the current range corresponding to the incomplete ZVS turn-on. We achieve all this using a single inductance value. Moreover, we delegate the junction temperature control to an external heat exchanger. This allows us to keep the switching frequency at a level corresponding to the target application and switching loop layout. The frequency can also be kept constant and at a low magnitude. With relatively low switching frequency we do not have a need for a high-bandwidth current sensor.

A. Electrical measurement principle

Generalised power MOSFET switching energies are shown in fig. 2. Traditionally, only the hard switching regime is shown in transistor datasheets. This is due to the fact that the soft switching behaviour is dependent on the deadtime and other system factors.

In order to measure different components of the losses the current in the DUT is controlled to achieve turn-on and turn-off at specific current levels (fig. 3). The experiment is divided into two measurement sets, focusing on turn-off and turn-on losses, respectively.

1) Turn-off losses: First a I_{ZVS} turn-on boundary current is calculated based on the energy levels stored in the output capacitances of the MOSFETs. Below this current level the transistor will turn-on lossless.

$$I_{ZVS} = I_{SW(ZVS)} = -\frac{2}{t_d}\int_0^{V_{DC}} C_{oss}(v)\mathrm{d}v \tag{1}$$

With the ZVS turn-on boundary established, the turn-on current is set below the I_{ZVS} and the turn-off current is swept, as in fig. 3a. For each I_{off} point we measure the total power loss P_{tot} in the DUT.

$$P_{tot} = \left(E_{on} + E_{cond} + E_{off}\right) \cdot f_{sw} \tag{2}$$

The conduction energy can be calculated as an integral of power dissipated in the DUT. The $i_D(t)$ information is needed. To obtain that, without affecting the switching loop, we measure the inductor current $i_L(t)$, which is equal to $i_D(t)$ when the DUT is on. The drain-to-source voltage is obtained using the static characteristic of the DUT.

$$E_{cond} = \int_{t_{on}}^{t_{off}} u_{DS}(i_D, T_j) \cdot i_D \, \mathrm{d}t \tag{3}$$

Knowing the conduction energy and assuming the turn-on energy is zero (full ZVS turn-on), we can then calculate the turn-off energies, using eq. 2.

2) Turn-on losses: The first measurement set gives us the turn-off energies as a function of the turn-off current. With that knowledge we set the turn-off current, for which we know the turn-off energy, and we sweep the turn-on current (as shown in fig. 3b).

Similar to the E_{off} extraction, we need to measure the total losses dissipated in the DUT and subtract the conduction and turn-off losses to obtain the turn-on losses.

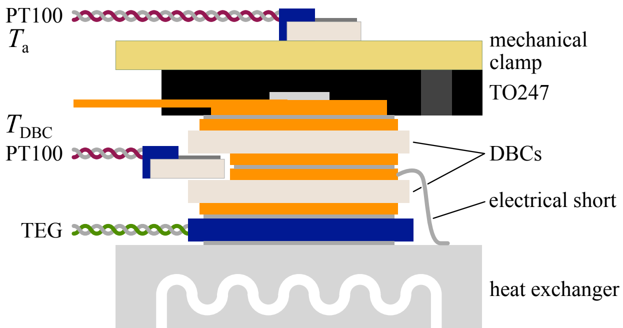

Fig. 4. Calorimetric measurement fixture cross-section.

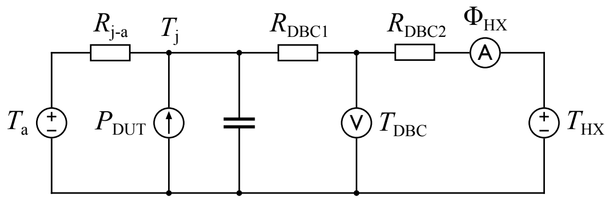

Fig. 5. Simplified thermal model of the fixture.

B. Calorimetric measurement setup

Both the turn-on and turn-off loss extraction require the measurement of the total losses extracted in the DUT.

The utilised calorimetric measurement fixture, shown in fig. 4 is a stack with two DBCs and a TEG thermoelectric heat flux sensor [8]. The sensor is measuring a fixed cross-section area, therefore a simple scaling is used to measure the heat passing through it.

A PT100 platinum temperature sensor is placed between the DBCs in an etched groove in the adjacent copper layers.

The heat flux sensor, during nominal operation, gives an output in the range of millivolts. To prevent any capacitive parasitic current flowing through the heat flux sensor the layer between the DBCs is shorted to the heat exchanger and serves as an EMI shield.

The heat flux sensor together with a temperature sensor and a thermal network model (fig. 5) can be used to estimate the junction temperature and power loss of the DUT.

In practice, not all DUT losses will be measured by the sensor. Some part of the DUT losses will leak to ambient through the pins and case of the DUT and some through the test fixture elements before the heat flux sensor. To minimise the error connected to this mechanism, authors strongly suggest to operate the circuit in a climate controlled environment.

To calibrate the fixture, static characteristics of the DUT anti-parallel diode are first measured at various temperatures ambient. Data should be collected using pulse measurement to minimise self heating.

Next, we inject a known magnitude of power (using a Kelvin connection) into the body diode of the DUT. Using the previously measured static characteristics we can quantify the junction temperature.

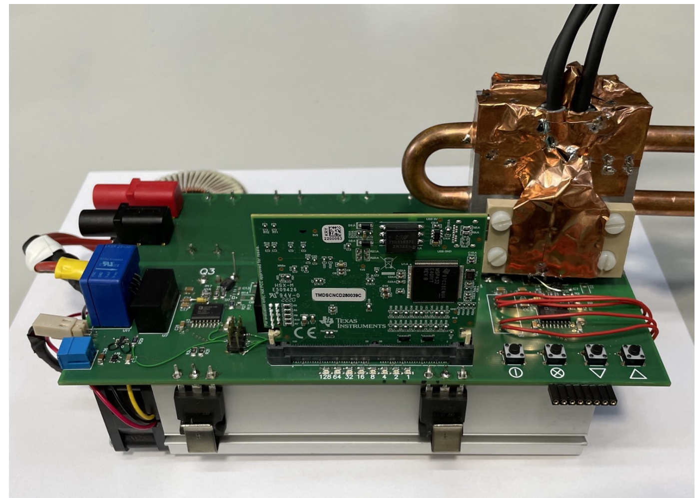

Fig. 6. A full-bridge measurement circuit with calorimetric measurement fixture mounted on the DUT.

By injecting various power magnitudes at different heat exchanger temperatures and ambient temperatures, we can then calibrate the fixture by obtaining the relationship between the measured $\{T_{\mathrm{DBC}}, T_{\mathrm{a}}, \Phi_{\mathrm{HX}}\}$ and $\{P_{\mathrm{DUT}}, T_{\mathrm{j}}\}$. Once this relationship is known, we can use the set of $\{T_{\mathrm{DBC}}, T_{\mathrm{a}}, \Phi_{\mathrm{HX}}\}$ to estimate the power dissipated in the DUT and its junction temperature while the DUT is operated in the full-bridge circuit.

III. Measurements

The calorimetric measurement fixture (fig. 4) was attached to the DUT in a full-bridge converter (fig. 6). For proof-of-concept operation the converter was operated at 20kHz at 50V DC-link voltage and 300ns deadtime. The IPW65R125C7 CoolMOS was used as the DUT. For these parameters the I_{ZVS} value is calculated, according to eq. 1, as -1.5A. The DC link voltage is well below the nominal operating range for this transistor, therefore the results do not represent the nominal performance of that transistor. It is, however, sufficient to demonstrate the applicability of the measurement method.

The presented results are measured with the test fixture and the converter placed inside a climate control chamber with T_{a} set to 25°C and with heat exchanger temperature T_{HX} also set to 25°C. The sensor was calibrated with power dissipated in the body diode and the resulting calibration curve was then used to convert sensor readings to the actual dissipated loss. The junction temperature was not controlled in the experiment but the estimated junction temperature for the operating points was not exceeding 30°C. Therefore, the biggest source of error for the presented data, was the estimation of u_{DS}.

The total switching energy broken down into corresponding E_{on}, E_{off} and E_{cond} for both turn-off and turn-on measurement sets is presented in figures 7 and 8, respectively. The turn-on and turn-off energies are extracted from the two measurement sets and shown in fig. 9.

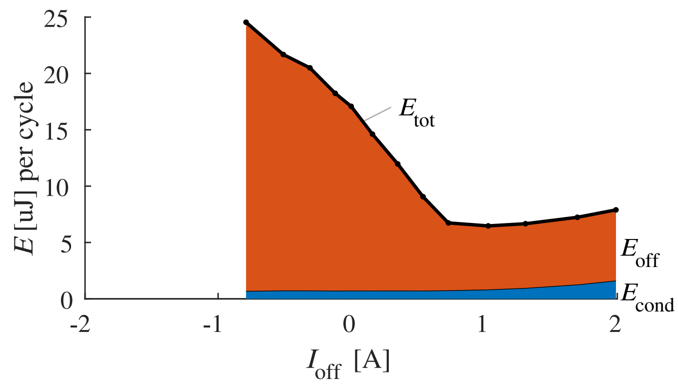

Fig. 7. Results of turn-off losses measurement set. Turn-on current level is set at -2A (less than I_{ZVS}) for all measured points, therefore, no E_{on} component is present in the breakdown.

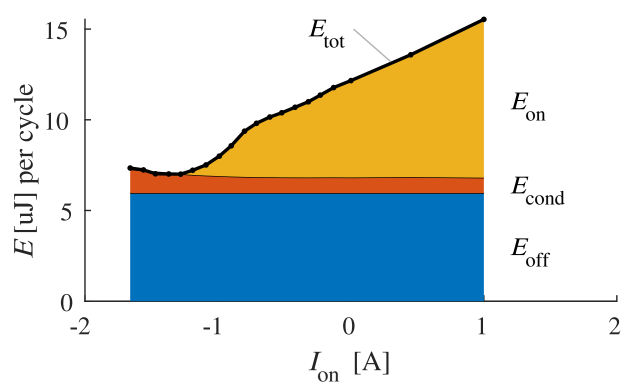

Fig. 8. Results of turn-on losses measurement set. Turn-off current level is set at $+2$A for all measured points. Note zero E_{on} component at currents less than $I_{ZVS} = -1.5$A.

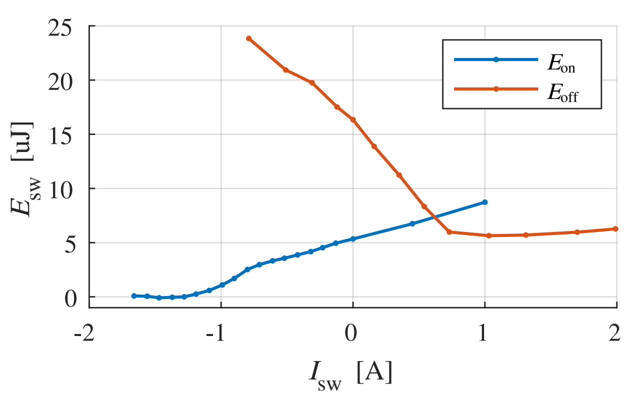

Fig. 9. E_{on} and E_{off} energies extracted from the experimental data shown in figures 7 and 8.

The turn-on energy plot shows a nearly linear behaviour in the hard-switching domain (for $I_{SW} > 0$). Full soft switching is achieved around -1.5A turn-on current. There is a soft transition in the iZVS area. This is due to the low DC voltage used in the experiment. Owing to the nonlinear C_{oss} capacitance, if a higher DC voltage was used, the $E_{on}(I_{on})$ function would tend towards almost a piecewise linear function with a step around $I_{ZVS}/2$ value. It stems from the fact that the i_L current needs to recharge the output capacitances of both top and bottom devices in the converter leg. As the voltage on one device falls, it raises on the complementary device with the sum of voltages equal to U_{DC}. At the point where the drain-to-source voltages are equal on both devices the output current sees the smallest total capacitance and the change in mid-point voltage is the steepest.

The turn-off energy shape shows a small positive slope at positive turn-off currents. This is a behaviour that is commonly seen in datasheets.

The turn-off energy also shows unexpected behaviour with negative currents, where E_{off} changes linearly, but with much higher slope than with positive current. Granted, a turn-off at negative current is rarely used in practice. Nonetheless, the behaviour is unexpected. At negative drain currents the turn-off of the channel should be lossless because the current will be commutated to the body diode of the DUT. The complementary device would then hard switch. The body diode of the DUT will experience some loss due to reverse recovery phenomena. This loss should be current dependent. Moreover, the conduction of the current through the body diode during the deadtime will be seen as a switching loss in this method. All this could explain the slope of the turn-off losses at negative switch currents.

In figure 9 the turn-off losses change the slope at $+0.75$A. The authors have confirmed that this point corresponds to $-I_{ZVS}/2$ value (note the I_{ZVS} is negative). When the deadtime was increased by 50% the kink in the $E_{off}(I_{SW})$ characteristics shifted accordingly. What is not obvious is the loss mechanism in the $0 \ldots -I_{ZVS}/2$ range. As the body diode is not activated during the deadtime for positive I_{SW} current, the only loss mechanism in the DUT is the product of i_D and u_{DS} during the deadtime period.

To explain the shape of the $E_{off}(I_{SW})$ function, in the $0 \ldots -I_{ZVS}/2$ range, we should examine what happens with the DUT's complementary switch. For small positive I_L currents, the complementary device is in the iZVS range. That means the value of u_{DS} at turn-off instant of the DUT depends on I_{SW}. DUT's E_{off} losses comprise of two components: the integral of product of u_{DS} and i_D during the deadtime, and hard switch losses when the transistor switches with the voltage remaining at u_{DS} at the end of the deadtime period. For low I_{SW} values both these components are significant and are current dependent. This mechanism was not observed in the data presented by Anderson et al.

IV. Conclusions

Using the presented method we have shown that extraction of E_{on} and E_{off} can be done for both positive and negative switch currents. This allows us to investigate both the hard- and soft-switching regimes.

Quantifying the incomplete soft-switching losses will allow the designers to accurately predict losses in the transistors. Currently many designs rely on the ZVS boundary as the limit of operation. Moving the boundary to the actual thermal limit of the converter, by exploiting the iZVS range, will allow more optimised power converter designs.

Prior studies into transistor losses mostly use an indirect power loss measurement. The heat flux sensor gives us access to a more direct, compact sensing unit.

The calorimetric fixture, as a whole, has proven to be difficult to use in practice. Multiple calibration steps are necessary to make accurate measurements. First, the DUT's static characteristics need to be characterised in first and third quadrants. This calibration needs to be performed at the expected junction temperature range. Next, a fixture calibration needs to be performed covering possible ambient temperatures, heat exchanger temperatures and possible dissipated powers. Due to the slow thermal time constants this calibration is time consuming. Any change to the physical setup invalidates the calibration.

Hence, for the measurements presented here, the authors have decided to simplify the measurement, minimise the possible error sources and measure with constant T_{a} and T_{HX} at low power levels. Obviously, if the losses were more significant, the T_{j} control would be necessary. Keeping the measurement circuit inside the climate controlled chamber removes the ambient temperature from the equation and shortens the required calibration times.

The method operates using a standard full-bridge converter and the DUT operates in an unmodified converter leg, therefore real world switching dynamic is preserved. No u_{DS} voltage sensor is necessary for the operation of the method. This means the capacitance of the half-bridge midpoint is preserved. The method can therefore measure the impact of any parasitic capacitance added to the switching node.

References

[1] P. Salmen, M. W. Feil, K. Waschneck, H. Reisinger, G. Rescher, and T. Aichinger, "A new test procedure to realistically estimate end-of-life electrical parameter stability of SiC MOSFETs in switching operation," in *2021 IEEE International Reliability Physics Symposium (IRPS)*, 2021.

[2] W. J. de Paula, G. H. M. Tavares, G. M. Soares, P. S. Almeida, and H. A. C. Braga, "Switching losses prediction methods oriented to power MOSFETs–a review," *IET Power Electronics*, vol. 13, no. 14, pp. 2960–2970, 2020.

[3] S. K. Roy and K. Basu, "An Energy based Approach to Calculate Actual Switching Loss for SiC MOSFET from Experimental Measurement," in *2021 IEEE 12th International Symposium on Power Electronics for Distributed Generation Systems (PEDG)*, 2021, pp. 1–5.

[4] X. Zhang, Z. Feng, J. Wang, and S. Yu, "An optimized temperature sensor calorimetric power device loss measurement method," *Energies*, vol. 12, no. 7, p. 1333, 2019.

[5] A. Anurag, S. Acharya, and S. Bhattacharya, "An Accurate Calorimetric Loss Measurement Method for SiC MOSFETs," *IEEE Journal of Emerging and Selected Topics in Power Electronics*, vol. 8, no. 2, pp. 1644–1656, 2020.

[6] J. A. Anderson, C. Gammeter, L. Schrittwieser, and J. W. Kolar, "Accurate Calorimetric Switching Loss Measurement for 900V 10 mΩ SiC mosfets," *IEEE Transactions on Power Electronics*, vol. 32, no. 12, pp. 8963–8968, 2017.

[7] L. Keuck, N. Jabbar, F. Schafmeister, and J. Böeker, "Switching loss characterization of wide band-gap devices by an indirect identification methodology," in *2018 20th European Conference on Power Electronics and Applications (EPE'18 ECCE Europe)*. IEEE, 2018, pp. P–1.

[8] *gSKIN® Heat Flux Sensors for R&D*, Greenteg, gSKIN XI 26 9C.